Classification of Sensory Neural Signals through Deep Learning Methods

Elisa Vasta
Department of Electronics, Information and Bioengineering
Politecnico di Milano
Milan, Italy
elisa.vasta@mail.polimi.it

Antonio Coviello
Department of Electronics, Information and Bioengineering
Politecnico di Milano
Milan, Italy
antonio.coviello@polimi.it

Umberto Spagnolini
Department of Electronics, Information and Bioengineering
Politecnico di Milano
Milan, Italy

Maurizio Magarini
Department of Electronics, Information and Bioengineering
Politecnico di Milano
Milan, Italy

***Abstract*— The recording and analysis of peripheral neural signals can be beneficial to provide feedback to prosthetic limbs and recover the sensory functionality in people with nerve injuries. Nevertheless, the interpretation of sensory recordings extracted from the nerve is not trivial, and only few studies have applied classifiers on sequences of neural signals without previous feature extraction. This paper evaluates the classification performance of two deep learning (DL) models (CNN and ConvLSTM) applied to the electroneurographic (ENG) activity recorded from the sciatic nerve of rats. The ENG signals, available from two public datasets, were recorded using multi-channel cuff electrodes in response to four sensory inputs (plantarflexion, dorsiflexion, nociception, and touch) elicited in response to mechanical stimulation applied to the hind paw of the rats. Different temporal lengths of the signals were considered (2.5 s, 1 s, 500 ms, 200 ms, and 100 ms). Both the two DL models proved to correctly discriminate sensory stimuli without the need of hand-engineering feature extraction. Moreover, ConvLSTM outperformed state-of-the-art results in classifying sensory ENG activity (more than 90% F1-score for sequences greater than 500 ms), and it showed promising results for real-time application scenarios.**

Keywords*— *ENG signals, classification, neural networks, deep learning, sensory stimulus, sciatic nerve.

I. Introduction

About 60’000 new cases of peripheral nerve injuries are reported every year just in the USA [1]. This type of damage can result in the complete or partial loss of sensory perception and movement control, altering the quality of life of the individuals. Recent research has seen the development of neuro prostheses as interfaces with peripheral nerves to incorporate sensory feedback and recover the lost functionalities [2-4]. These devices aim at bypassing the injury and restoring the flow of information between the central nervous system and the rest of the body. Among all, bidirectional devices are the best solutions because they can both record and later stimulate peripheral nerves in order to deliver sensory feedback [5,6]. A schematic of the functioning of main blocks implementing the sequence of operations in a neuro prosthesis interface is shown in Fig. 1. Such a system acquires the electrical signals from both ends of the peripheral nerve damage, send them to an external computer, interprets them and artificially stimulates the nerve, thus creating a bypass that can mimic the physiological response of the body.

Fig. 1. Block diagram of operations in a bidirectional neuro prosthesis.

Neuro prostheses for the open-loop control of lower and upper limb movement has improved in recent years [7,8], but the incorporation of sensory feedback within these devices is still challenging. Electromyographic (EMG) signals are usually employed for prosthetic movement control since they are easily accessible, but they cannot provide sensory information [9]. Thus, directly recording and interpreting ENG signals at the level of the nerve can guarantee better neuro-prosthesis performance, exploiting the neurosensory path of the patient. While advances have been achieved in stimulating peripheral nerves and producing sensory perceptions [7,8,10], the ability of long-term recording of ENG signals has not been thoroughly investigated. The main problems are the low Signal-to-Noise Ratio (SNR), the biocompatibility of the acquisition system and the poor surgical accessibility of the nerve [11-13]. With regards to the acquisition system, extra neural cuff electrodes, which act as sensors wrapped around the nerve, are often considered the preferable option to measure the ENG activity thanks to their low invasiveness. However, one of their main drawback is the limited SNR and selectivity compared to intraneural electrodes [13]. Thus, the direct interpretation of sensory information recorded from the nerve is not trivial, also because of the high complexity of the neural system. Indeed, the “transfer function” among the acquired ENG activity and the expected output is unknown. Therefore, neuro protheses should comprise a classification algorithm that can learn from past values of the recorded signal and generate data-driven predictions.

In this context, the main contribution of this work is the introduction of deep learning classifiers for the discrimination of four sensory stimuli (touch, dorsiflexion, plantarflexion, and nociception) from ENG signals. In particular:

- two classification approaches that can deal with noisy data without the need of hand-engineering feature extraction were evaluated. The novelty is the introduction of the ConvLSTM model, which is particularly suitable for spatio-temporal data and for extracting long-term temporal relationships within

the signal. The second model is based on Convolutional Neural Networks (CNN), state-of-the-art classifiers for spatiotemporal data, thus allowing performance comparison;

- focus was dedicated to evaluate the influence of the implantation site for the electrical contacts on the discrimination performance;
- five different temporal lengths of ENG sequences were evaluated to identify the optimal ones for both off-line and real-time classification scenarios. In the latter case, the acquisition plus the classification time intervals should be strictly less than 300 ms, which is the acceptable and not perceivable time delay between the stimulation of the limb and the actual classification of the signal [14].

The paper is organized as follows. Section 2 discusses related works on the classification of sensory evoked ENG signals. The proposed approaches for processing and classifying the data are introduced in Section 3. In Section 4, we present the main results and their discussion. Section 5 concludes the paper and delineates future research.

II. Related works

Most of the algorithms implemented so far for the classification of sensory ENG signals require a preliminary extraction of features, which can be obtained by the Running Observation Window (ROW) method [9]. It consists in sliding a fixed time window (∼100/300 ms) over the ENG sequence to compute a set of selected characteristics, such as the mean absolute value, the wavelength or the variance estimator [15]. Later, a machine learning model employs such features to discriminate the sensory input that evoked the ENG activity. The main classifiers analyzed in sensory discrimination tasks are Linear Discriminant Analysis (LDA) [9], Support Vector Machines (SVM) [11,16,17], and Random Forest. Brunton et al. [16] employed a ROW-based approach to classify different sensory stimuli (e.g., nociception, touch, proprioception) from the ENG signals using SVM, reporting ∼83% mean accuracy. Moreover, Silveira *et al.* [18] applied LDA in separating 10 different stimuli, achieving up to 65% in the best-performing animal. The results of [18] also indicate that placing the cuff electrode in the distal position on the sciatic nerve allows to achieve a better discrimination of sensory stimuli compared to the proximal position. An important aspect of ROW is the possibility to perform majority voting to avoid transient jumps after the classification of sensory stimuli in each window [11].

Recently, novel feature extraction frameworks have also been investigated. These comprise the spatio-temporal focus and the dynamic time warping to reduce the computational cost and improve the classification performance. The Spatio-Temporal Warping (STW) approach, introduced by Silveira *et al.* [9] before the LDA classifier, allowed to discriminate six proprioceptive stimuli with accuracy between 93.4 and 98%. On the other hand, other studies focused on the Velocity Selective Recording (VSR) to exploits the temporal information within ENG signals [19,20], like the conduction velocity and the direction of propagation of the electrical activity inside the nerve. Moreover, it is possible to infer the firing rate of active neural fibers within the nerve by detecting the compound action potentials (CAPs), i.e. the signature activity of the simultaneous activation of multiple neurons. Thus, its firing rate, as well as its shape, can be attributed to a different sensory stimulus. Koh *et al.* [21] were the first at introducing an innovative approach for ENG classification based on a combination of the CAP detection and the VSR method. They fed individual detected CAPs to an Artificial Neural Network (ANN) and a CNN architecture. The algorithms reached about 76.10% mean accuracy and 68.40% mean F1 score for separating dorsiflexion from plantarflexion, whereas the results were lower when trying to also separate the pricking stimulus.

Even though the feature extraction process is still the most common approach, it can be time-consuming, and it requires human expert dependency for selecting the most relevant characteristics [22]. In this context, deep learning frameworks are getting more attention because they can handle and classify raw signals without the need of previous data processing steps. As for the feature extraction methods, most of the techniques adopted for ENG signal classification have been previously employed in the analysis of EMG activity, like CNN [23], ANN [24], Spiking Neural Network (SNN) [25] and Recurrent Neural Network (RNN) [26]. In a recent work, Porta et al. [27] obtained almost 84% mean accuracy in discriminating ten different stimuli (touch, nociception, dorsiflexion and plantarflexion at different intensities) with both CNN and SNN. Even better results were found when merging labels belonging to the same sensorial type (∼97% mean accuracy on the best animal). RNN architectures were not implemented for ENG classification so far, but they showed promising results in EMG-based applications, like recognition of finger and hand gestures [26], prosthesis control [28], and gait pattern recognition in exoskeletons [29].

III. Datasets and methodologies

The classification task of sensory nerve responses in rats was performed on two different datasets made available by the Newcastle University. The first one, the dataset 1, was produced in August 2016 [16]; the second one, the dataset 2, was acquired from November 2016 to May 2017 and later analyzed in [18]. The two datasets contain measures of naturally evoked ENG signals obtained by mechanical stimulation of the limb of five Sprague Dawley rats (three in dataset 1 and two in dataset 2). Extra-neural 16-channels cuff electrodes were positioned on the sciatic nerve of the animals (4 rings of 4 platinum contacts each), in distal position for dataset 1 and in proximal position for dataset 2 (see Fig. 2). The acquisition of the ENG signals was carried out with sampling frequency of 30 kHz. In particular, different classes of sensory stimuli were administered to the rats' hind paw, grouped into the following stimulus categories:

- nociception, with two classes depending on the pinching locations on the foot: heel pinch and outer toe pinch;
- proprioception, which subsequentially divides in plantarflexion (+10°, +20°, +30°) and dorsiflexion (-10°, -20°, -30°) of the ankle with respect to a neutral position, for a total number of 6 classes;
- touch, with two stimuli related to different ways of touching the animal (100 g and 300 g of force). The experimental setup planned to alternate the stimulation with resting time instants (Fig. 2a).

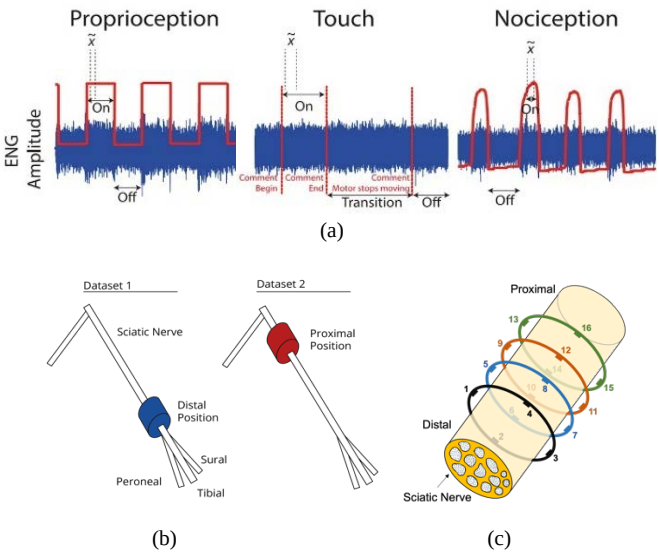

Fig. 2. ENG signal (blue) and synchronization signal (red) for the different stimulus categories (a) [16]; different positions of cuff electrodes in the datasets (b) and the configuration of the electrodes in the 16-channel cuff (c).

A. Signal Processing

Before feeding the data to the classifiers, the signals were preprocessed to reduce some intrinsic problems, using MATLAB™. The main negative impairments affecting the data are:

- *powerline interference (PLI)*, which is present in all the recordings, with most contribution in the lowest harmonics;
- *sampling jitter-based distortions*, which is visible in the time-frequency domain due to the acquisition system.

The PLI was not removed from the signals, but suitable classifiers that can handle noisy data were selected. On the other hand, the regridding technique described in [27] was carried out to fix the uneven time grid of the signals. Starting from the Short Time Fourier Transform (STFT) of the ENG signals, it is possible to quantify the sampling shift $\Delta f_s(t)$ as:

$$\Delta f_s(t) \approx -f_{s0} \cdot \frac{\Delta f_0(t)}{f_0} \qquad (1)$$

where f_{s0} is the nominal sampling frequency (30kHz) and $\Delta f_0(t)$ is the estimated shift of one PLI harmonic at its real frequency f_0. The harmonic at 750 Hz was selected to estimate $\Delta f_0(t)$ because it was the one presenting the highest peak in the Power Spectral Density (PSD). Then, the actual time instants in which the signal was sampled were derived. More details of this method are given in [27].

Later, an 8th-order Butterworth bandpass filter between 800 Hz and 2450 Hz was applied to obtain the ENG bandwidth of interest. Besides, noisy timesteps of the signal (up to some voltage) were deleted because they completely alter the ENG activity and its discrimination. Time instants higher than a 30 mV in one or more electrodes were deleted. Finally, the signal was downsampled from 30 kHz to 5 kHz to reduce the dimensionality of the data.

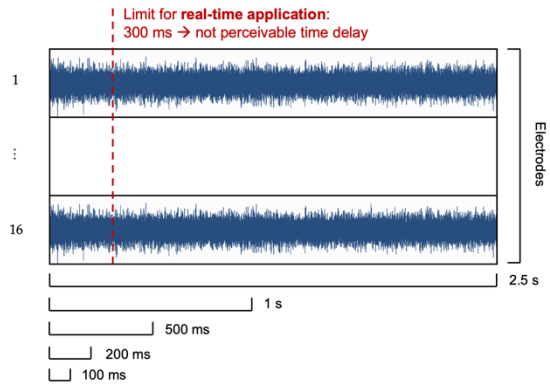

Fig. 3. Scheme of the different ENG sequence lengths.

B. ENG sequence preparation

Sequence length correction. The sequences corresponding to the stimulation instants were obtained using the synchronization signals in Fig. 2a). The ENG sequence lengths were not constant, either within the same trial or in different sensory stimuli. Sequences duration were about 3 s both in dataset 1 and 2 for proprioception and touch, whereas the nociceptive sequences varied significantly in length: 0.25 s- 1.40 s (dataset 1) 1.8 s- 5.6 s (dataset 2). Thus, the final sequence length was set to 2.5 s to standardize, considering only the steady-state response to mechanical stimulation as already carried out in previous works [16]. Truncation (for longer sequences) or padding same (for shorter sequences) was applied.

Final dataset correction. A different number of repetitions were found for each stimulus class. Moreover, few sequences were too noisy, so they were discarded from the analysis. The final dataset is shown in Table 1, which is lightly unbalanced. Finally, the labels of each sequence were one-hot encoded for feeding the classifiers.

TABLE 1. *Final number of ENG sequences*

Animal	**Type of stimulation**			
	Nociception	***Plantarflexion***	***Dorsiflexion***	***Touch***
1	129	150	150	100
2	104	145	147	78
3	103	150	147	98
4	102	177	177	79
5	89	144	148	97

C. Classification setup

The classifiers were evaluated on different classification setups with varying time lengths of the ENG sequences (2.5 s, 1 s, 500 ms, 200 ms and 100 ms), exploiting the available data as much as possible (see Fig. 3).

Thus, from each sequence of 2.5 s more samples were obtained according to the chosen window. Moreover, different models were implemented for different animals, due to the inter-subject variability. Stratified 5-fold cross-validation was carried out to avoid the presence of overfitting. The sets were stratified also considering the different stimulus intensities and not only the 4 main sensory types, i.e., touch, nociception,

dorsiflexion, and plantarflexion. Two models were considered: ConvLSTM which was evaluated on all the sequence lengths, and CNN, which was implemented as a comparison only on two selected sequence lengths (500 ms and 200 ms). Two different metrics were selected: the accuracy and the F1-score (macro). The first is the most used metric in ENG classification problems, so the results will be more comparable with the state-of- the-art. The second also considers the minority class instances and it was obtained by averaging the F1-scores of each class.

D. Classification models

CNNs networks are usually applied to structured spatio-temporal inputs because of their ability to recognize patterns within data without the need of feature extraction. For this reason, in this work a convolutional architecture was employed and adapted from [27]. It comprises a combination of two 1D convolutional layers: one with a kernel $E \times 1$ along the dimension of the electrodes and the other with kernel $1 \times K$ for convolving the signal in the time dimension. The result of these convolutions is then summed together row-by-row along the time dimension. Each of the kernels was moved with a stride length of 1, and padding "same" was applied to maintain the same dimensionality after the convolution. These layers form a convolutional block. Four convolutional blocks with an increasing number of filters (32, 64, 126, 256) were inserted before two simple 1D CNN layers, a flatten layer and a fully connected layer performing the classification. Max-pooling and dropout layers were used after each convolutional layer for dimensionality reduction and preventing overfitting respectively. A rectified linear unit (ReLu) activation function was employed in each convolutional layer to introduce non-linearity, whereas Softmax was used at the end to transform the unbounded outputs into probabilities.

The second model is the ConvLSTM, usually applied in video classification tasks. ConvLSTM was selected for its ability to extract spatio-temporal patterns typical of the CNN and at the same time understand temporal relationships within "frames" of ENG signals, as the Long-Short Term Memory (LSTM) [30]. In standard LSTM, the core cell can store values over arbitrary time periods thanks to three gates, that control the information flow into and out of the cell (Fig. 4). New knowledge is accumulated when the input gate is activated, and previous cell status is forgotten if the forget gate is active. Finally, the output gate decides if the final state should propagate. In the case of ConvLSTM, the convolution operator is also applied to the inputs. Unlike normal LSTM that can handle only 1D data, ConvLSTM takes 3D inputs, like the width, the height, and the RGB channels in an image. In this work, the samples of ENG signal to classify were transformed in a video-like structure: each sequence was divided into more time windows of length M and height 16, which is the number of electrodes, and these windows are handled as "frames" (Fig. 4). The value of M was chosen empirically and set to 20 ms. The ConvLSTM architecture in this work comprises three main blocks, with a convolutional and a max pooling layers, before a final flatten and dense layers. The number of filters was set to 16, 32 and 64 for blocks in ascending order, whereas the kernel size to 11 for the temporal dimension and 3 for the "electrode"

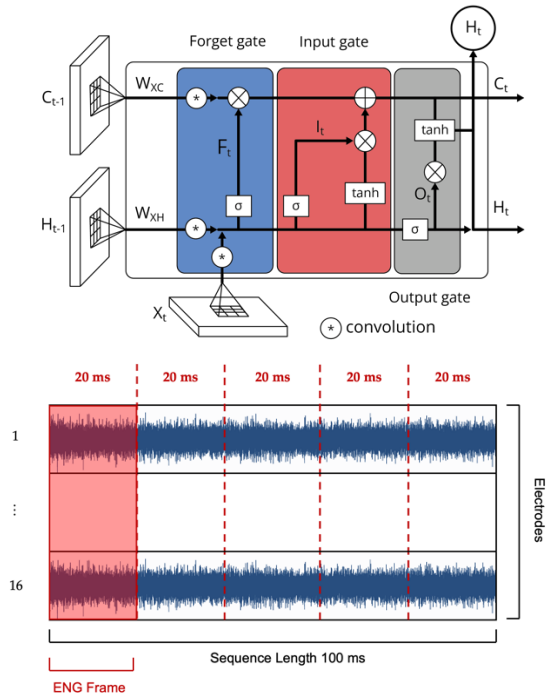

Fig. 4. Scheme of the ConvLSTM cell (up) and representation of the "ENG frames" of 20 ms within a sequence (100 ms) to classify (down).

dimension. The recurrent drop out, which is the fraction of the units to drop at each iteration for the linear transformation of the recurrent state, was 0.2.

TABLE II. *Results of the ConvLSTM (mean F1-score), reported as mean ± standard deviation calculated in the testing phase of the 5-fold cross-validation.*

Sample length	**F1-score (%)**				
	Animal 1	***Animal 2***	***Animal 3***	***Animal 4***	***Animal 5***
2.5 s	98.9 ±1.5	91.1 ±8.2	79.2±12.8	37.8 ±4.8	66.3 ±4.0
1 s	92.2 ±4.7	86.8 ±6.0	91.8 ±4.9	31.7 ±6.7	78.3±17.2
500 ms	92.7 ±1.9	94.5 ±2.6	87.7 ±3.2	42.7 ±3.3	69.8 ±2.8
200 ms	90.1 ±3.5	77.6 ±1.8	81.8 ±1.5	42.7 ±2.9	62.9 ±5.8
100 ms	85.6 ±0.9	75.9 ±1.0	76.6 ±2.2	40.7 ±1.7	65.3 ±1.6

IV. RESULTS AND DISCUSSION

Table II shows the results in terms of mean F1-score obtained by the ConvLSTM model in the various setups, whereas the accuracy is reported in the boxplots (Fig. 5). The averaged results among animals in dataset 1 indicated that the ConvLSTM can discriminate the 4 different sensory stimuli with ~90% mean accuracy and mean F1-score among animals for sequence length of 2500 ms, 1000 ms and 500 ms, ~83% for 200 ms and ~79% for 100 ms. On the other hand, for dataset 2 the averaged outcomes among rats are almost constant for all the setups, ranging between 51% and 56% approximately. With the available datasets, the optimal trade-off between performance and repeatability was also identified. Sequence length of 500 ms should be selected for off-line classification. Instead, if one aims at incorporating the sensory discrimination into a real-time

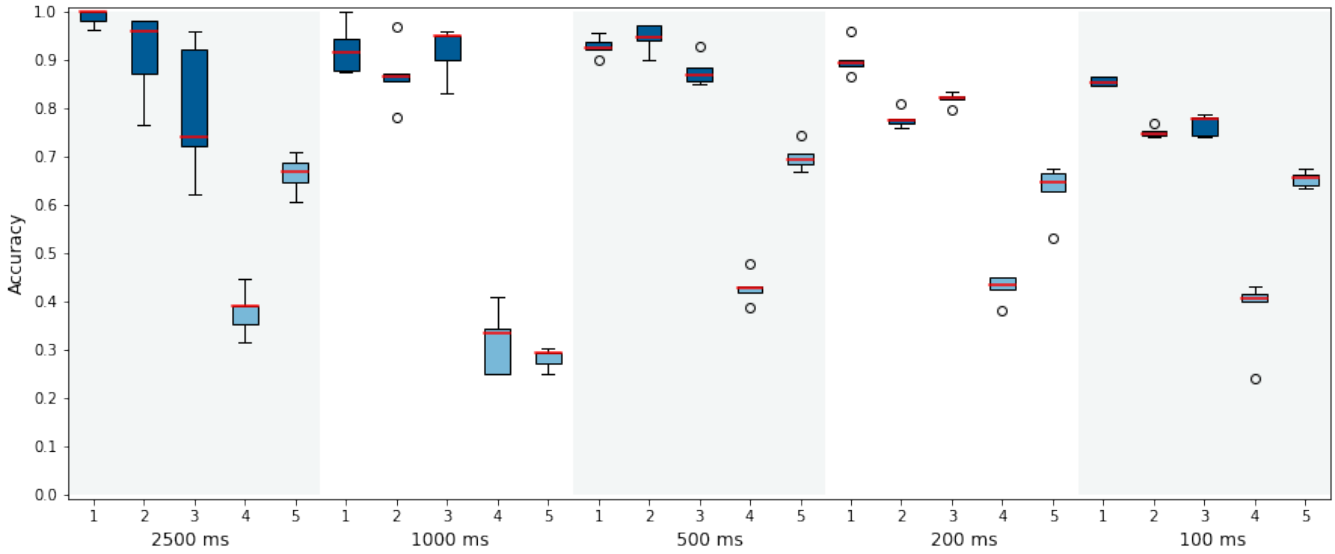

Fig. 5. Boxplots of the overall results (accuracy) of ConvLSTM during the 5-fold CV. Animals 1, 2 and 3 of dataset 1 are in blue, animals 4 and 5 of dataset 2 are in light blue to indicate the different implantation sites of the cuff-electrode.

device, the choice falls on 200 ms, which is lower than the acceptable and non- perceivable time delay (300 ms).

As far as the comparison with the CNN is concerned, the mean F1-scores are reported in Table III. The ConvLSTM performed almost 10% better than the CNN architecture for the 500 ms setup, where this latter reached about 81% averaged accuracy and F1-score among animals. For the 200 ms case, the CNN results are almost 5% lower compared to the ConvLSTM. At the same time, the results are comparable to the ConvLSTM for the 500 ms classification task (~55%) in dataset 2 and they are slightly better for sequence length of 200 ms.

TABLE III. *Results of the CNN (F1-score), reported as mean ± standard deviation calculated in the testing phase.*

Sample length	**F1-score (%)**				
	Animal 1	***Animal 2***	***Animal 3***	***Animal 4***	***Animal 5***
500 ms	90.2 ±5.0	80.8 ±4.2	72.4 ±2.8	43.3 ±4.4	65.1±15.4
200 ms	87.4 ±4.5	72.3 ±3.4	74.0 ±8.3	44.7 ±2.4	68.9±14.3

From the results of both CNN and ConvLSTM, an appreciable difference in performance can be noticed between dataset 1 and dataset 2. Indeed, the cuff electrodes were implanted in different positions: distally in the sciatic nerve for animal 1, 2 and 3 and proximally for animal 4 and 5. This corroborated previously findings that the implantation site of the cuff-electrode on the proximal part of the sciatic nerve allows to discriminate sensory stimuli less compared to the distal position [18]. For dataset 2, most of the misclassifications happened between the dorsiflexion and the plantarflexion, most likely due to the anatomy of the sciatic nerve. The increase in fasciculation in the distal position guarantees better classification performance because the cuff electrode can acquire the signals with higher selectivity. Furthermore, it can be observed all the testing models obtained different performance with respect to the animal considered. In dataset 1, rat 1 was the best performing in almost every setup, whereas in dataset 2 the classifiers discriminated sensory signal better in rat 5. The inter-subject variability is due to some stochastic factors, such as the positioning of the cuff electrode, the electrode coupling with the nerve, micro damages caused by the surgery, the nerve orientation with respect to the electrodes or the physiological nature of the ENG signals [11,18]. All these aspects contribute to affect the SNR, thus the final classification performance.

Finally, the results of the ConvLSTM architecture were compared with the state-of-the-art. For dataset 1, Porta et al. [27] obtained similar averaged results among animals on 1s ENG sequences, but the ConvLSTM outperforms their CNN (above 94% accuracy) when comparing the maximal performance in every animal. Moreover, they conducted a hard signal processing, which suggests that the ConvLSTM method can handle noisy data while preserving the same performance without the need of a time-consuming processing. For dataset 2, LDA classifiers were tested in [18], using sequence length of 2.5 s for touch and proprioception and 500 ms for nociception. The maximum accuracy and F1-score in the animal 4 were 42.9% and 41.3%, which are lower than the maximal performance obtained by the ConvLSTM on 2.5 s or on 500 ms sequences. Moreover, both accuracy and F1-score were largely lower compared to animal 5, which in our case reached better results than animal 4.

V. CONCLUSIONS

In this work, the ConvLSTM model for discriminating sensory stimuli from the ENG activity in the sciatic nerve was successfully introduced. First, a light signal processing pipeline was selected before the actual classification task, pointing towards the realization of a real-time sensory discrimination method. The signals were down sampled even to 5 kHz before the classification, proving that it is possible to obtain high performance even with lower sampling frequencies. Then, two different models, ConvLSTM and CNN, were chosen because they do not require previous hand-engineering feature extraction and they can handle noisy data. Two publicy available datasets were considered for this analysis. Two optimal sequence lengths were found for off-line (500 ms) and real-time (200 ms) application scenarios. For animals in dataset 1, the ConvLSTM

performed ~10% better than the CNN with time length of 500 ms and almost 5% better with 200 ms sequences. Instead, both models reached comparable performance in dataset 2. All the results confirmed prior findings that cuff electrodes in the distal position on the sciatic nerve can enhance the discrimination of sensory stimuli compared to the proximal site. Moreover, the superiority of the ConvLSTM for the classification task was proved with respect to the state-of-the-art.

ACKNOWLEDGMENT

We would like to thank Federica Porta and the PNRelay group. At the same time, all the authors express their thanks to the researchers of the Newcastle University for sharing their datasets.

REFERENCES

[1] N. Y. Li, G. I. Onor, N. J. Lemme, and J. A. Gil, 'Epidemiology of Peripheral Nerve Injuries in Sports, Exercise, and Recreation in the United States, 2009 – 2018', *Phys. Sportsmed.*, vol. 49, no. 3, pp. 355–362, Jul. 2021, doi: 10.1080/00913847.2020.1850151.

[2] G. Valle, A. Saliji, E. Fogle, A. Cimolato, F. M. Petrini, and S. Raspopovic, 'Mechanisms of neuro-robotic prosthesis operation in leg amputees', *Sci. Adv.*, vol. 7, no. 17, p. eabd8354, Apr. 2021, doi: 10.1126/sciadv.abd8354.

[3] K. Nazarpour, A. Krasoulis, and J. M. Hahne, 'Control of prosthetic hands', in *Control of Prosthetic Hands: Challenges and emerging avenues*, K. Nazarpour, Ed. Institution of Engineering and Technology, 2020, pp. 1–13. doi: 10.1049/PBHE022E_ch1.

[4] D. W. Tan, M. A. Schiefer, M. W. Keith, J. R. Anderson, J. Tyler, and D. J. Tyler, 'A neural interface provides long-term stable natural touch perception', *Sci. Transl. Med.*, vol. 6, no. 257, Oct. 2014, doi: 10.1126/scitranslmed.3008669.

[5] I. Williams *et al.*, 'SenseBack - An Implantable System for Bidirectional Neural Interfacing', *IEEE Trans. Biomed. Circuits Syst.*, vol. 14, no. 5, pp. 1079–1087, Oct. 2020, doi: 10.1109/TBCAS.2020.3022839.

[6] S. Raspopovic *et al.*, 'Restoring Natural Sensory Feedback in Real-Time Bidirectional Hand Prostheses', *Sci. Transl. Med.*, vol. 6, no. 222, Feb. 2014, doi: 10.1126/scitranslmed.3006820.

[7] T. Callier and S. J. Bensmaia, 'Restoring the sense of touch with electrical stimulation of the nerve and brain', in *Somatosensory Feedback for Neuroprosthetics*, Elsevier, 2021, pp. 349–378. doi: 10.1016/B978-0-12-822828-9.00010-1.

[8] B. Güçlü, 'Introduction to somatosensory neuroprostheses', in *Somatosensory Feedback for Neuroprosthetics*, Elsevier, 2021, pp. 3–40. doi: 10.1016/B978-0-12-822828-9.00022-8.

[9] C. Silveira, R. N. Khushaba, E. Brunton, and K. Nazarpour, 'Spatio-temporal feature extraction in sensory electroneurographic signals', *Philos. Trans. R. Soc. Math. Phys. Eng. Sci.*, vol. 380, no. 2228, p. 20210268, Jul. 2022, doi: 10.1098/rsta.2021.0268.

[10] G. Preatoni, F. Dell'Eva, G. Valle, A. Pedrocchi, and S. Raspopovic, 'Reshaping the full body illusion through visuo-electro-tactile sensations', *PLOS ONE*, vol. 18, no. 2, p. e0280628, Feb. 2023, doi: 10.1371/journal.pone.0280628.

[11] S. Raspopovic, J. Carpaneto, E. Udina, X. Navarro, and S. Micera, 'On the identification of sensory information from mixed nerves by using single-channel cuff electrodes', *J. NeuroEngineering Rehabil.*, vol. 7, no. 1, p. 17, Dec. 2010, doi: 10.1186/1743-0003-7-17.

[12] B. P. Christie *et al.*, '"Long-term stability of stimulating spiral nerve cuff electrodes on human peripheral nerves"', *J. NeuroEngineering Rehabil.*, vol. 14, no. 1, p. 70, Dec. 2017, doi: 10.1186/s12984-017-0285-3.

[13] C. E. Larson and E. Meng, 'A review for the peripheral nerve interface designer', *J. Neurosci. Methods*, vol. 332, p. 108523, Feb. 2020, doi: 10.1016/j.jneumeth.2019.108523.

[14] T. R. Farrell and R. F. Weir, 'The Optimal Controller Delay for Myoelectric Prostheses', *IEEE Trans. Neural Syst. Rehabil. Eng.*, vol. 15, no. 1, pp. 111–118, Mar. 2007, doi: 10.1109/TNSRE.2007.891391.

[15] K. Englehart, B. Hudgins, P. A. Parker, and M. Stevenson, 'Classification of the myoelectric signal using time-frequency based representations', *Med. Eng. Phys.*, vol. 21, no. 6–7, pp. 431–438, Jul. 1999, doi: 10.1016/S1350-4533(99)00066-1.

[16] E. Brunton, C. Blau, C. Silveira, and K. Nazarpour, 'Identification of sensory information in mixed nerves using multi-channel cuff electrodes for closed loop neural prostheses', in *2017 8th International IEEE/EMBS Conference on Neural Engineering (NER)*, Shanghai, May 2017, pp. 391–394. doi: 10.1109/NER.2017.8008372.

[17] E. Brunton, C. W. Blau, and K. Nazarpour, 'Separability of neural responses to standardised mechanical stimulation of limbs', *Sci. Rep.*, vol. 7, no. 1, p. 11138, Dec. 2017, doi: 10.1038/s41598-017-11349-z.

[18] C. Silveira, E. Brunton, S. Spendiff, and K. Nazarpour, 'Influence of nerve cuff channel count and implantation site on the separability of afferent ENG', *J. Neural Eng.*, vol. 15, no. 4, p. 046004, Aug. 2018, doi: 10.1088/1741-2552/aabca0.

[19] M. Schuettler, V. Seetohul, J. Taylor, and N. Donaldson, 'Velocity-Selective Recording from Frog Nerve Using a Multi-Contact Cuff Electrode', in *2006 International Conference of the IEEE Engineering in Medicine and Biology Society*, New York, NY, Aug. 2006, pp. 2962–2965. doi: 10.1109/IEMBS.2006.260335.

[20] J. Taylor, B. Metcalfe, C. Clarke, D. Chew, T. Nielsen, and N. Donaldson, 'A Summary of Current and New Methods in Velocity Selective Recording (VSR) of Electroneurogram (ENG)', in *2015 IEEE Computer Society Annual Symposium on VLSI*, Montpellier, France, Jul. 2015, pp. 221–226. doi: 10.1109/ISVLSI.2015.34.

[21] R. G. L. Koh, A. I. Nachman, and J. Zariffa, 'Use of spatiotemporal templates for pathway discrimination in peripheral nerve recordings: a simulation study', *J. Neural Eng.*, vol. 14, no. 1, p. 016013, Feb. 2017, doi: 10.1088/1741-2552/14/1/016013.

[22] S. Raspopovic *et al.*, 'Neural signal recording and processing in somatic neuroprosthetic applications. A review', *J. Neurosci. Methods*, vol. 337, p. 108653, May 2020, doi: 10.1016/j.jneumeth.2020.108653.

[23] R. G. L. Koh, M. Balas, A. I. Nachman, and J. Zariffa, 'Selective peripheral nerve recordings from nerve cuff electrodes using convolutional neural networks', *J. Neural Eng.*, vol. 17, no. 1, p. 016042, Jan. 2020, doi: 10.1088/1741-2552/ab4ac4.

[24] A. David Orjuela-Canon, A. F. Ruiz-Olaya, and L. Forero, 'Deep neural network for EMG signal classification of wrist position: Preliminary results', in *2017 IEEE Latin American Conference on Computational Intelligence (LA-CCI)*, Arequipa, Nov. 2017, pp. 1–5. doi: 10.1109/LA-CCI.2017.8285706.

[25] E. Donati, M. Payvand, N. Risi, R. Krause, and G. Indiveri, 'Discrimination of EMG Signals Using a Neuromorphic Implementation of a Spiking Neural Network', *IEEE Trans. Biomed. Circuits Syst.*, vol. 13, no. 5, pp. 795–803, Oct. 2019, doi: 10.1109/TBCAS.2019.2925454.

[26] P. Koch, H. Phan, M. Maass, F. Katzberg, and A. Mertins, 'Recurrent Neural Network Based Early Prediction of Future Hand Movements', in *2018 40th Annual International Conference of the IEEE Engineering in Medicine and Biology Society (EMBC)*, Honolulu, HI, Jul. 2018, pp. 4710–4713. doi: 10.1109/EMBC.2018.8513145.

[27] A. Coviello, F. Porta, M. Magarini, and U. Spagnolini, 'Neural network-based classification of ENG recordings in response to naturally evoked stimulation', in *Proceedings of the 9th ACM International Conference on Nanoscale Computing and Communication*, Barcelona Catalunya Spain, Oct. 2022, pp. 1–7. doi: 10.1145/3558583.3558855.

[28] H. Aly and S. M. Youssef, 'Bio-signal based motion control system using deep learning models: a deep learning approach for motion classification using EEG and EMG signal fusion', *J. Ambient Intell. Humaniz. Comput.*, Jul. 2021, doi: 10.1007/s12652-021-03351-1.

[29] C. Chen, Z. Du, L. He, Y. Shi, J. Wang, and W. Dong, 'A Novel Gait Pattern Recognition Method Based on LSTM-CNN for Lower Limb Exoskeleton', *J. Bionic Eng.*, vol. 18, no. 5, pp. 1059–1072, Sep. 2021, doi: 10.1007/s42235-021-00083-y.

[30] C. Shi, Z. Zhang, W. Zhang, C. Zhang, and Q. Xu, 'Learning Multiscale Temporal–Spatial–Spectral Features via a Multipath Convolutional LSTM Neural Network for Change Detection With Hyperspectral Images', *IEEE Trans. Geosci. Remote Sens.*, vol. 60, pp. 1–16, 2022, doi: 10.1109/TGRS.2022.3176642.